Environ Monit Assess (2021) 193: 507
https://doi.org/10.1007/s10661-021-09281-x

Monitoring of land use/land cover changes using GIS and CA-Markov modeling techniques: a study in Northern Turkey

Hasan Aksoy · Sinan Kaptan

Received: 15 April 2021 / Accepted: 12 July 2021 / Published online: 23 July 2021

Abstract The purpose of this study, covering the northern Ulus district of Turkey, was to analyze the forest and land use/land cover (LULC) changes in the past period from 2000 to 2020, and to predict the possible changes in 2030 and 2040, using remote sensing (RS) and geographic information systems (GIS) together with the CA–Markov model. The maximum likelihood classified (MLC) technique was used to produce LULC maps, using 2000 and 2010 Landsat (ETM+) and 2020 Landsat (OLI) images based on existing stand-type maps as reference. Using the historical data from the generated LULC maps, the LULC changes for 2030–2040 were predicted via the CA-Markov hybrid model. The reliability of the model was verified by overlapping the 2020 LULC map with the 2020 LULC model (predicted) map. The overall accuracy was found to be 80.90%, with a Kappa coefficient of 0.74. The total forest area (coniferous + broad-leaved + mixed forest) grew by 10,656.4 ha (15.4%) in the 2000–2020 period. Examination of the types within the Forest Class revealed that the coniferous forest area had grown by 5.9% in the period 2000–2010, whereas it had decreased by 4.7% in the period 2010–2020. The broad-leaved forest area had grown by 1.2% and 3.1%, respectively, between 2000 and 2010 and 2010 and 2020. The mixed forest area had been reduced by 7.1% in the period 2000–2010 but had grown by 1.7% in the 2010–2020 period. In the Non-Forest Class, although the water area had increased in the 2000–2020 period, agricultural land and settlement areas had decreased by 11,553.9 ha (32.3%) and 34.6 ha (0.5%), respectively. According to the 2020–2040 LULC simulation results, it was predicted that there would be 3.8% and 26.4% growth in the total forest and water surface areas and 13.9% and 5.3% reduction in the agricultural and settlement areas, respectively. Using the LULC simulation to separate the Forest Class into coniferous, broad-leaved, and mixed forest categories and subsequently examining the individual changes can be of great help to forest planners and managers in decision-making and strategy development.

Keywords CA-Markov · Simulation · GIS · Forest cover change · LULC · Turkey

H. Aksoy (✉)
Department of Forestry and Forest Products, Ayancık Vocational School, Sinop University, 57402 Sinop, Turkey
e-mail: haksoy@sinop.edu.tr

S. Kaptan
Department of Forest Management and Planning, Faculty of Forestry, Bartın University, 74100 Bartın, Turkey

Introduction

Land use/land cover (LULC) changes are an important factor in natural resource management and sustainable development (Degife et al., 2018; Hou et al., 2019; Motlagh et al., 2020; Ren et al., 2019). These changes occur mainly as a result of the anthropogenic effects of deforestation, urbanization, destruction of rangelands, reduction of wetlands, etc. (Akinyemi et al., 2017; Moradi et al., 2020; Niya et al., 2020). The LULC changes directly affect ecology, land degradation, and climate and have been found to negatively affect ecosystem services and functions on a regional and global scale (Karki et al., 2018; Khwarahm et al., 2020; Tolessa et al., 2017). These ecosystem alterations have gradually increased awareness of the importance of LULC changes on a global scale (Rohde, 2013; Steffen et al. 2006; Carpenter et al., 2009; Akinyemi, 2017). Understanding these problems arising from LULC changes, their causes, and effects is a topic that has attracted the attention of researchers in many parts of the world. In particular, those working on temporal and spatial land transformation models have shown great interest in LULC changes (Keshtkar & Voigt, 2016; Keshtkar et al., 2017; Wu et al., 2008). Models of LULC used in describing the causes and consequences of LULC changes have become useful tools in the study of future landscape changes, land management, and in the pre-evaluation of proposed policies (Ren et al., 2019; Schulp et al., 2008; Verburg & Overmars, 2009).

In recent years, the different spatial and temporal coverage of satellite systems, with their high resolution and increased data supply capabilities, have increased the use of their images in tracking LULC changes. All these positive developments have made remote sensing (RS) data a critical input for LULC classification studies (Khwarahm et al., 2020). In particular, Landsat images have been widely used for identification and monitoring LULC changes, as they provide 40 years of relatively high spatial resolution ground observation data at no cost (Gómez et al., 2016; Khwarahm et al., 2020; Li et al., 2020; Pflugmacher et al., 2019; Zhu & Woodcock, 2014). In addition to the data obtained with RS, there have been positive developments in the integration of auxiliary data into Geographic Information Systems (GIS) (Ball, 1994), and integrating Markov modeling into GIS has made it possible to transform LULC change studies from a specific pattern to a specific process (Weng, 2002). The cellular automata (CA)-Markov model can be efficiently integrated with GIS and RS. It is a robust approach that can be used in dynamic modeling of land-use changes in temporal and spatial terms (Kamusoko et al., 2009; Sang et al., 2011). The GIS and RS data contribute greatly to the creation of next-year scenarios by providing tools to define the initial conditions of CA-Markov, parameters of the model, calculation of transition probabilities, and determination of the neighborhood rules (Wang & Zhang, 2001). Therefore, CA-Markov hybrid models, especially those based on LULC changes over past years, are frequently used in studies to determine possible future situations (Da Cunha et al., 2021). It is possible to come across many international studies in which LULC change scenarios have been successfully predicted using the CA–Markov model (Aburas et al., 2021; Khawaldah et al., 2020; Khwarahm, 2021; Mondal et al., 2016; Munthali et al., 2020; Rimal et al., 2019; Ruben et al., 2020; Salem et al., 2020; Singh et al., 2015).

Forest areas, having the widest distribution among the terrestrial ecosystems, automatically provide many products and services, especially carbon storage, via their own natural processes. Forestry operations are known to be intensive in terms of labor, cost, and time, with their results and effects emerging after many years. Moreover, the recompense for unsuccessful enterprises is equally demanding, costly, and time-consuming. Demands for justification and concerns at the global, regional, and local scale necessitate the planning and supervision of forests in accordance with sustainable forest management (SFM) practices. The success of producing and implementing forest management plans depends on determining the most appropriate policies and strategies and making dependable decisions to ensure the realization of SFM. The identification of any changes provides the information needed in order to successfully determine conservation strategies for natural resources (Reddy et al., 2018) and to make healthier decisions in the use and management of natural resources (Akinyemi et al., 2017; Feng et al., 2020; Gharbia et al., 2016; Moradi et al., 2020). Consequently, monitoring, mapping, evaluating, and reporting the changes in forest areas and putting the necessary measures in place in a timely manner are of great importance.

The aim of this study, based on the years 2000, 2010, and 2020, was to examine the current LULC changes within the borders of the Ulus Forest Management Directorate via RS and GIS and to predict the probable LULC changes for 2030 and 2040 using simulations performed by the CA–Markov model. A total of six categories were analyzed. The Forest area classes included coniferous, broad-leaved, and mixed forest and the Non-Forest area classes comprised agriculture (arable land), settlement, and water. Thus, scenarios were developed to reveal possible changes and the direction and severity of these changes in coniferous, broad-leaved, and mixed forest areas in the coming years. To the authors' knowledge, to date, no study has been carried out examining LULC changes within the administrative borders of the Ulus Forestry Management Directorate and modeling future LULC scenarios using the CA-Markov approach. The information acquired will help decision-makers and managers to carry out forest planning in accordance with the principle of sustainability and to determine and develop consistent policies and strategies in this direction. In addition, monitoring the current changes for agriculture, settlement, and water areas in the Non-Forest area class and revealing possible changes for the coming years could contribute to urban and agricultural policy-making decisions.

Study area

The study was carried out in the Ulus district of Bartın Province situated in the Western Black Sea Region of Turkey. The study area consists of 112,460.22 ha within the Ulus FMD administrative boundaries. Ulus is located between 41° 50′ North latitude and 32° 57′ East longitude and is generally composed of rough terrain with an average altitude of 200 m a.s.l. The dominant vegetation of the area is forest. It is surrounded by the Black Sea in the north, Kastamonu in the east, Karabük in the southeast, and Zonguldak in the west (Anon, 2020). Ulus FMD consists of 10 plan units: Abdipaşa, Ardıç, Drahna, Hasandede, Kumluca, Merer, Samatlar, Sarıkaya, Sökü, and Ulusçayı (Fig. 1).

The annual average temperature is 12.8 ºC, and the annual precipitation is 1046.2 mm. The rainy and temperate climate structure and appropriate ecological conditions increase the variety of vegetation.

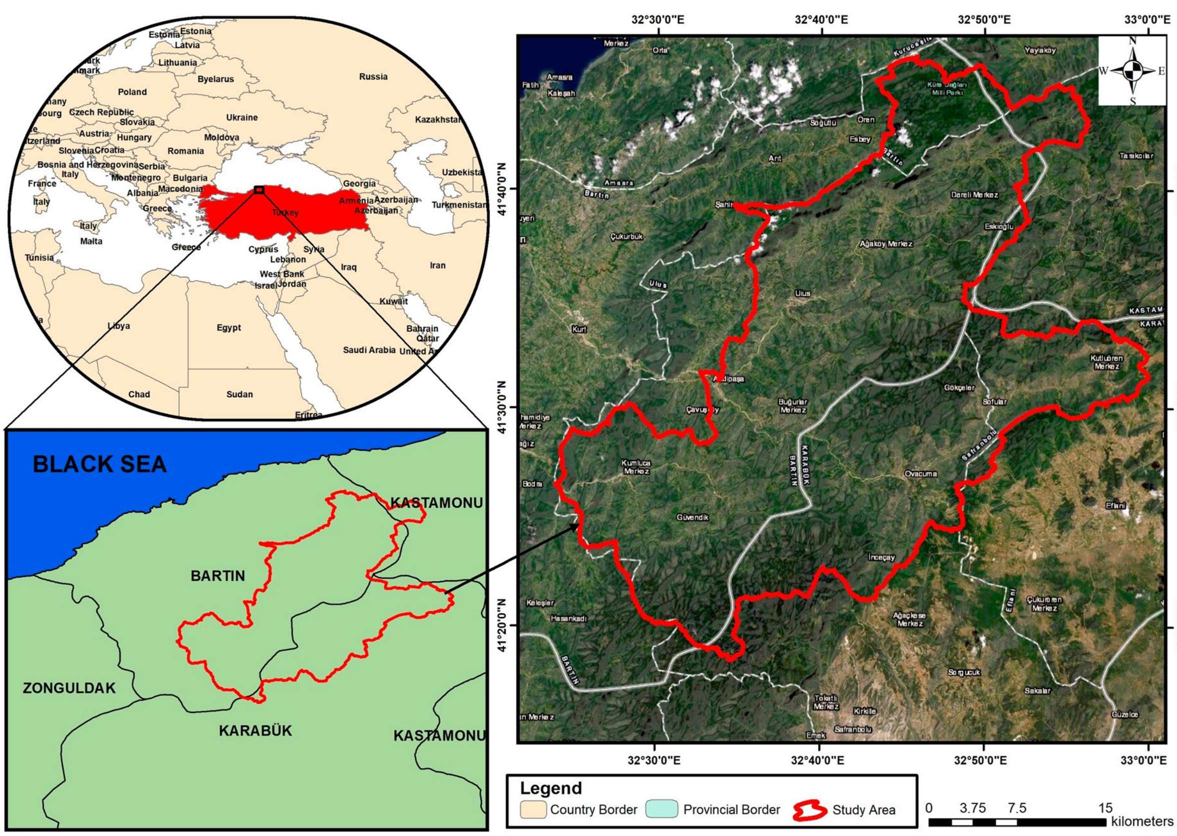

Fig. 1 Geographical location of the study area

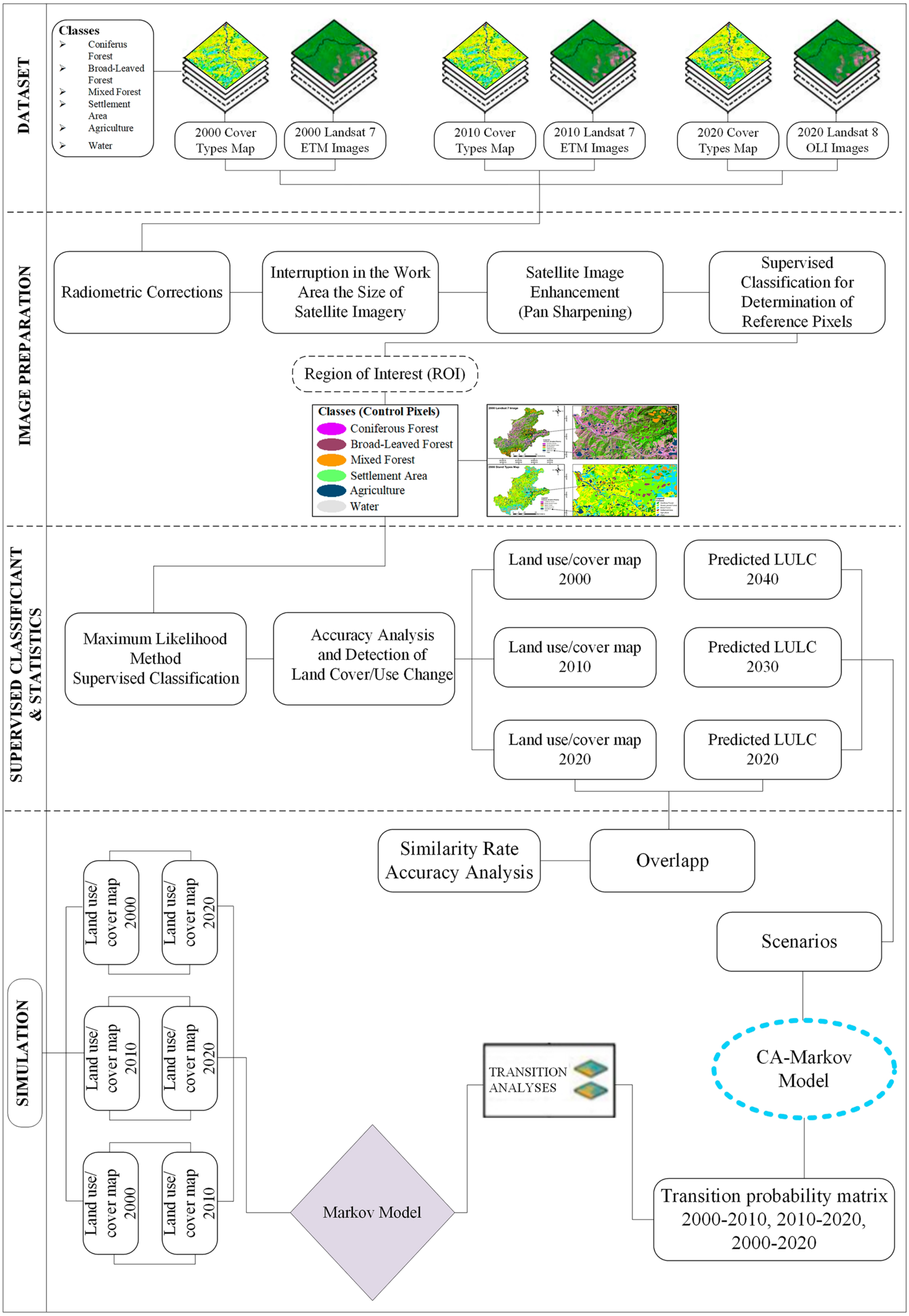
DATASET
Classes
Coniferus Forest
Broad-Leaved Forest
Mixed Forest
Settlement Area
Agriculture
Water
2000 Cover Types Map
2000 Landsat 7 ETM Images
2010 Cover Types Map
2010 Landsat 7 ETM Images
2020 Cover Types Map
2020 Landsat 8 OLI Images
IMAGE PREPARATION
Radiometric Corrections
Interruption in the Work Area the Size of Satellite Imagery
Satellite Image Enhancement (Pan Sharpening)
Supervised Classification for Determination of Reference Pixels
Region of Interest (ROI)
Classes (Control Pixels)
Coniferous Forest
Broad-Leaved Forest
Mixed Forest
Settlement Area
Agriculture
Water
SUPERVISED CLASSIFICIANT & STATISTICS
Maximum Likelihood Method Supervised Classification
Accuracy Analysis and Detection of Land Cover/Use Change
Land use/cover map 2000
Land use/cover map 2010
Land use/cover map 2020
Predicted LULC 2040
Predicted LULC 2030
Predicted LULC 2020
SIMULATION
Similarity Rate Accuracy Analysis
Overlapp
Scenarios
Land use/ cover map 2000
Land use/ cover map 2020
Land use/ cover map 2010
Land use/ cover map 2020
Land use/ cover map 2000
Land use/ cover map 2010
CA-Markov Model
TRANSITION ANALYSES
Markov Model
Transition probability matrix 2000-2010, 2010-2020, 2000-2020

◂**Fig. 2** Flowchart showing methodology of the study

Approximately 52% of the area is forest, generally consisting of broad-leaved and coniferous trees. The characteristic trees of the area up to 600 m high along the coastal side are *Quercus* sp., *Fagus* sp., and *Carpinus* sp. In areas toward the interior from the coast higher than 1500 m, *Fagus* sp., *Castanea* sp., *Abies* sp. and *Pinus* sp. are found, whereas along the coastal strip, *Juglans* sp. and *Corylus* sp. are common (Atik, 1998).

Material and methods

In this study, the supervised classification process was carried out for the images of Landsat-7 ETM + for 2000 and 2010 and Landsat-8 OLI images for 2020 with the stand-type maps of the relevant years taken reference. For the supervised classification process and accuracy analysis, ENVI software was used. The CA–Markov model was used to simulate the 2020 LULC changes over the map in the supervised classified images from 2000 to 2010. The accuracy of the model was verified by comparing the classified 2020 satellite image with the 2020 simulation map. After establishing the accuracy of the model, LULC simulation maps of the study area were produced for the years 2030 and 2040. The general methodological framework of the study is shown in Fig. 2.

Landsat satellite images

The Landsat ETM + images for 1999 and 2009 and Landsat 8 OLI/TIRS images for 2019 used in the study were taken from the United States Geological Survey (USGS) website. In order to perform the classification process with high accuracy, cloudless (< 10%) satellite images taken during the same season of the years 2000, 2010, and 2020 were used. The features of the satellite images used are shown in Table 1.

In order to distinguish the clearest LULC, the red (band 5), green (band 4), and blue (band 3) were used as the band combination, respectively, in the Landsat 7 ETM + images between 2000 and 2010. In the 2020 Landsat 8 OLI images, the red (band 6), green (band 5), and blue (band 4) were used, respectively. A standard deviation correction of 1% was applied as an image enhancement process. The satellite image was geographically referenced to a Universal Transverse Mercator coordinate system with region 36 north. The root mean square error (RMSE) of the georeferenced satellite image was less than one pixel. The atmospheric correction (ENVI) was then applied to the Landsat satellite images.

Stand-type maps

Stand-type maps for 2000, 2010, and 2020, which were taken as a reference base in the classification and simulation, were obtained from the Ulus FMD. The non-numerical stand-type maps from the past were digitized and recorded using ArcGIS. The production of stand-type maps is the first and most important step in creating the forest management plans that form the basis of Turkey's forestry work. These maps were produced as a result of a hierarchical process carried out according to the combined inventory method based on RS (satellite images or aerial photographs prepared at an appropriate scale) and ground measurements (Fig. 3).

The first stage of map production is to take aerial photographs of the forest planning unit at the appropriate scale and height. These photos are calibrated and interpreted by forest engineers who are experts in aerial photo interpretation. The forest stand types are separated, and 1/25,000-scale digital draft stand maps are created. Internal division projections are made on the draft maps and given to the planning team 1 year prior to the operations. In compliance with the legislation, the draft maps are finalized according to the local measurement results carried out by the relevant team in sample areas at specified intervals and distances (Aksoy & Kaptan, 2020).

Clipping satellite images according to the operating limits and image enhancement

In the study, a Composite Band process was applied for the 2000–2010 Landsat 7 ETM + and 2020 Landsat 8 OLI images. The composite band data created were clipped to fit the boundaries of the study area. First of all, the success of classification was directly proportional to the high quality and clarity of the images to be used. For this reason, an image enhancement process (Pan Sharpening) was applied

Table 1 Features of Landsat sensors and images used to classification (USGS, 2020)

Satellite	Date acquired	Path	Row	Spectral interval	Band width (µm)	Spatial resolution (m)
Landsat 7 ETM+	04 Jul 2000 13 May 2010	178	31	Band 1	0.45–0.51	30
				Band 2	0.53–0.61	30
				Band 3	0.63– 0.69	30
				Band 4	0.75–0.90	30
				Band 5	1.55–1.75	30
				Band 6	10.4–12.5	30
				Band 7	1.09–2.35	30
				Pan	0.52–0.90	15
Landsat 8 OLI/TIRS	3 Jul 2020	178	31	Band 1	0.43–0.45	30
				Band 2	0.45–0.51	30
				Band 3	0.53–0.59	30
				Band 4	0.64–0.67	30
				Band 5	0.85–0.88	30
				Band 6	1.57–1.65	30
				Band 7	2.11–2.29	30
				Band 8 (pank)	0.50–0.68	15

to increase the perceptibility, interpretability, quality, and nature of the images.

Determination of reference pixels

Two different classification methods are used in the image classification process: supervised and unsupervised. In the unsupervised classification method, when there is no information about an image, the classification is performed by creating clusters according to the spectral reflection value of the image. In the supervised classification method, classification is performed by referring to materials with spatial and objective information about the image. In the study, the supervised classification process was carried out on the satellite images of the relevant years by taking the Ulus FMD stand-type maps of 2000, 2010, and 2020 as reference.

To simulate and evaluate LULC changes, a total of six classification categories were defined: settlement, agricultural, and water areas in the Non-Forest Area class, and coniferous, broad-leaved, and mixed forests in the Forest Area class. Reference pixels required for the supervised classification process were determined according to the density and distribution of the land classes using stand-type maps for the years 2000, 2010, and 2020, GPS terrestrial measurement data, and high-resolution Google Earth images. Snedecor and Cochran (1969) used the number of reference pixels taken to determine the minimum number of sample pixels (Eq. 1):

$$N = 4pq/E \quad (1)$$

where N: total number of pixels to be sampled, p: expected percent accuracy, q: 100-p, E: maximum permitted error percentage.

As a result of the calculations, the minimum sample pixel count was determined as 204 for an accuracy rate of 85% with a 5% maximum error margin. The reference pixels were then overlapped with the satellite image, and the satellite images were classified based on the reflection values of the pixels corresponding to each class. The distribution of reference pixels on a stand-type map and on a satellite image is shown in Fig. 4.

The accuracy of the satellite images obtained as a result of the supervised classification was checked via ENVI software using the error matrix method based on reference pixels. The accuracy of the classified satellite images was verified using overall accuracy, producer accuracy, user accuracy,

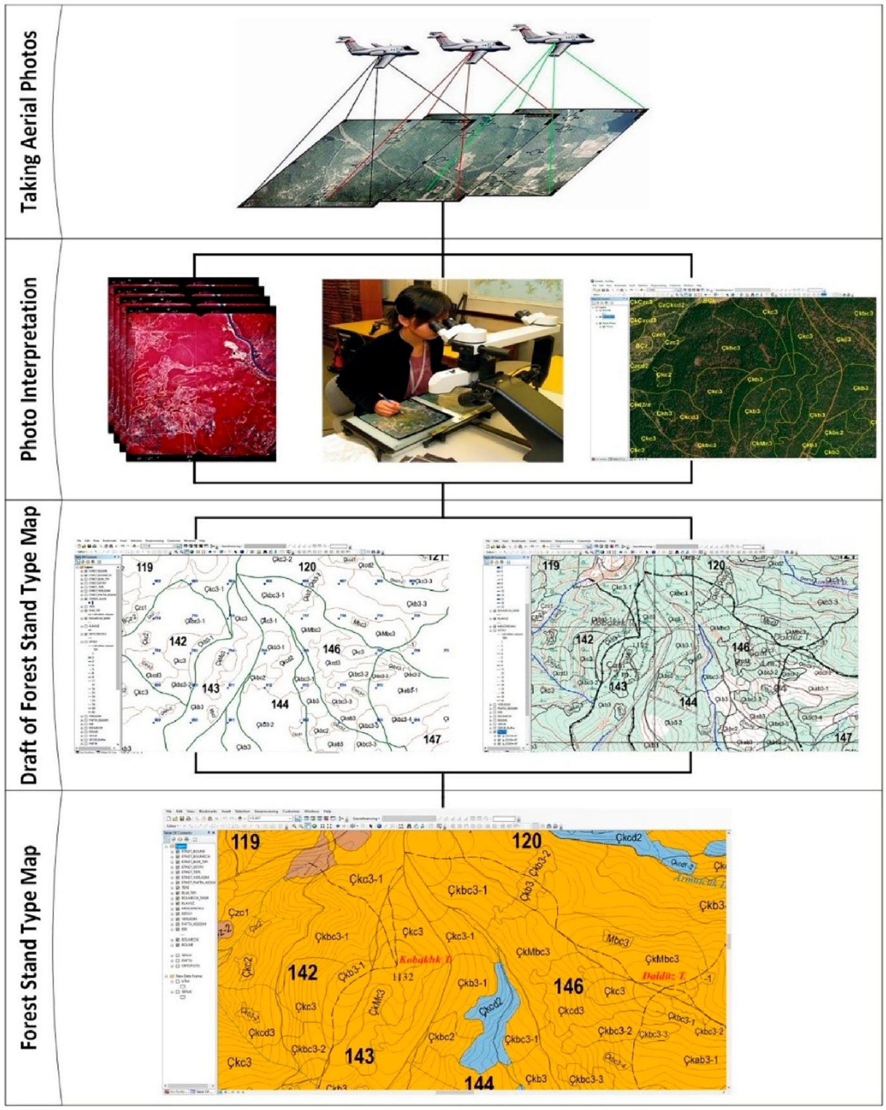

Fig. 3 Forest stand-type map production stages (Kaptan, 2021a)

and Kappa statistics values. Overall accuracy indicates the degree to which the obtained classification is compatible with the actual situation in the field, whereas producer accuracy shows how well each category is classified by the sample pixels. User accuracy shows how many pixels actually situated on the land of the user are accurately represented on the classified map. Finally, the Kappa coefficient (κ) shows the true fit between the reference data and the classified map (Congalton & Green, 2019).

Scenario modeling (cellular automaton-Markov model) and validation

The Markov chain is a model that uses the logic of applying the probability of transition to predict the next situation and all future situations depending on the current situation (Guan et al., 2008). This model incorporates the idea of simulating the next period based on the status of the previous period, using the inter-period change-transition probability matrix (Aksoy & Kaptan, 2020; Wang & Murayama, 2017).

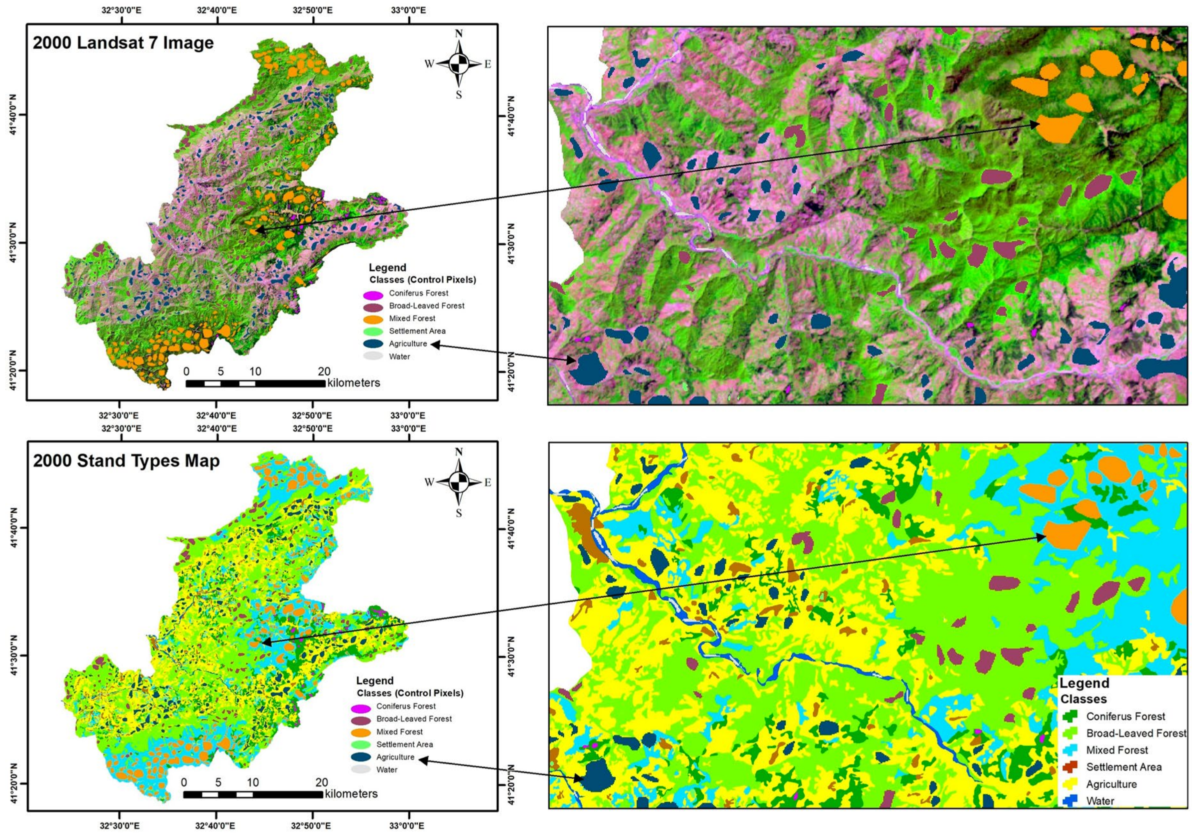

Fig. 4 Distribution of reference pixels

In this study, with the Markov process, the land-use model is equivalent to a situation at a given time, and the areas changing between land-use types represent the transition probability rate of the situation. Equation (2) shows the Markov prediction (Huang et al., 2020):

$$Z_{(l+1)} = Z_l \times Q \tag{2}$$

Here, $Z_{(1\,+\,1)}$ represents the LULC status at time $1+1$, whereas Z_1 indicates the LULC status; l represents time, and Q represents the probability matrix of transition from time l to the $l+1$ time frame:

$$Z = \left[Z_1\, Z_2 Z_3 Z_4 Z_5\, Z_6\right] \tag{3}$$

Here (Eq. 3), $Z_i (i = 1, 2, \ldots, 6)$ indicates coniferous forest, broad-leaved forest, mixed forest, residential areas, agricultural land, and water bodies and their usage areas; Q below can be defined as the $[n, n]$ matrix (Eq. 4):

$$Q = \begin{bmatrix} Q_{11} & Q_{12} & \cdots & Q_{1n} \\ Q_{21} & Q_{22} & \cdots & Q_{2n} \\ \vdots & \vdots & \vdots & \vdots \\ Q_{n1} & Q_{n2} & \cdots & Q_{nn} \end{bmatrix}, \sum\nolimits_{(j=1)}^{n} Q_{ij} = 1, 1 \le i,j \le n, n = 6 \tag{4}$$

Here, n is the total number of land-use patterns, Q_{ij} = indicates the possibility of transition from i to j in the land-use pattern, and the sum of each row of the matrix must be equal to "1".

The CA model is a discrete dynamic model that describes complex situations in nature and is used in the simulation of specific self-replicating situations within a living system (Wolfram, 1984). Compared to other dynamic models, CA consists of a set of rules and has the nature, rationality, and feasibility to simulate complex systems, and thus, it can simulate complex natural phenomena more clearly, accurately, and precisely (Itami, 1994). A standard CA model is divided into four concepts: a discrete cellular state (D), a finite state (S), a neighborhood (L), and rules

(R). According to a given transformation function, the next status of a cell is determined by the current status and its neighborhood. The four phases can be defined as follows:

$$CA = (D, S, L, R) \tag{5}$$

Here (Eq. 5), CA, D, S, L, and R are defined as the Cellular Automata system, the discrete state, the size of any positive integer, the neighborhood, and the rules, respectively.

In particular, L is calculated as in Eq. (6):

$$L = \left(S_1, S_2, S_3, \cdots, S_n\right), S_n \in S \tag{6}$$

Here, n is the number of neighbors (Huang et al., 2020).

The IDRISI TerrSet is a tool that can be used to derive the necessary data for use in these models, and it contains the modules required for the analysis and processing of spatial data.

For this reason, the CA and Markov chain analysis modeling of the LULC scenarios (2020, 2030, and 2040) carried out in the study was performed via the IDRISI TerrSet 17.0 software developed by Clark Labs. The period used in the CA/Markov chain analysis of change was then used as the starting point for the LULC change simulation for the year 2020. A standard 5×5 contiguity filter was applied to the forward projection for the number of cellular automata (CA) iterations specified in the Markov chain analysis, based on the amount of time elapsed.

Results

Image classification results

Based on LULC maps of 2000, 2010, and 2020, Landsat satellite images and using the stand-type maps of the relevant years as reference, supervised classification was performed showing the six categories of coniferous, mixed, and broad-leaved forests and settlement, agricultural, and water areas. Figure 5

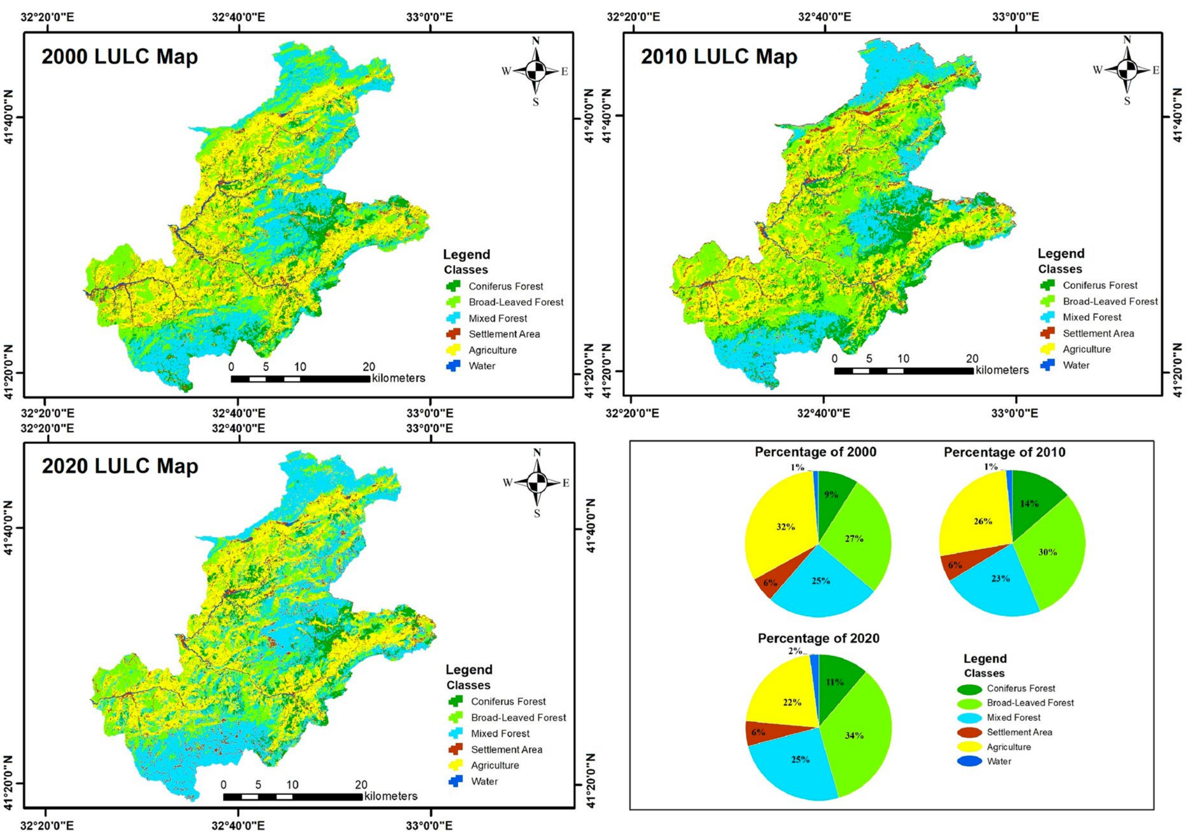

Fig. 5 Time series of LULC maps of Landsat ETM+and OLI supervised classified images of the study area (2000, 2010, and 2020)

shows the LULC maps produced for each period after classification.

Table 2 shows the success of the classification according to the accuracy values and error matrices of the LULC maps obtained as a result of the classification. The reference pixel numbers and area (ha) values of each class are directly proportional. The water class, with the smallest area value in all 3 years in terms of reference pixel numbers, is classified with the least pixel value on the 2010 LULC map (1063 pixels).

For the year 2000 LULC map, the overall accuracy was 86.56% and the Kappa coefficient, which shows statistically the accuracy of the supervised classification and its ability to represent the study area, was 0.81. The highest producer accuracy values (≥ 80%), respectively, belonged to the coniferous forest, broad-leaved forest, mixed forest, and agriculture classes. The lowest producer accuracy (41.69%) was shown for the settlement class. The user accuracy rate was above 80% for all classes except those of the coniferous forest (78.56%) and settlement (30%) classes (Table 2).

Table 2 Error matrix and accuracy values of supervised classified images (2000, 2010, and 2020)

Accuracy and error matrix values of Landsat ETM and OLI supervised classified images (2000, 2010, and 2020)

	Coniferous	**Broad-leaved**	**Mixed**	**Settlement**	**Agriculture**	**Water**	**Total**	**User's accuracy (%)**
2000								
Coniferous	5430	215	769	57	376	65	6,912	78.56
Broad-leaved	59	23,038	835	142	971	170	25,215	91.37
Mixed	266	759	12,575	3	24	0	13,627	92.28
Settlement	32	211	18	951	1,301	679	3,192	29.79
Agriculture	26	1264	2	1,061	20,646	625	23,624	87.39
Water	11	13	1	67	95	2,562	2,749	93.20
Total	5824	25,500	14,200	2281	23,413	4,101	75,319	–
Producer's accuracy (%)	93.23	90.35	88.56	41.69	88.18	62.47	–	–
Overall accuracy = 86.567%; Kappa coefficient 0.81								
2010								
Coniferous	9,703	9	355	8	0	0	10,075	96.31
Broad-Leaved	174	21,394	525	258	850	32	23,233	92.08
Mixed	1074	590	11,811	26	6	1	13,508	87.44
Settlement	14	155	57	2772	447	85	3530	78.53
Agriculture	4	237	0	342	16,741	28	17,352	96.48
Water	6	44	11	100	18	884	1,063	83.16
Total	10,975	22,429	12,759	3,506	18,062	1,030	68,761	–
Producer's accuracy (%)	88.41	95.39	92.57	79.06	92.69	85.83	–	–
Overall accuracy = 92.065%; Kappa coefficient 0.89								
2020								
Coniferous	7,350	59	586	13	145	3	8,156	90.12
Broad-Leaved	74	21,034	2,136	12	418	1	23,675	88.84
Mixed	1345	1,495	45,217	69	183	3	48,312	93.59
Settlement	236	94	840	2,539	594	327	4,630	54.84
Agriculture	436	520	657	651	16,362	564	19,190	85.26
Water	19	0	3	152	29	1,999	2,202	90.78
Total	9460	23,202	49,439	3436	17,731	2897	106,165	–
Producer´s accuracy (%)	77.70	90.66	91.46	73.89	92.28	69	–	–
Overall accuracy = 89.013%; Kappa coefficient 0.84								

For the 2010 LULC map, the overall accuracy rate was 92.06% and the Kappa coefficient was 0.89. User accuracy was above 80% for all classes except for the settlement area class (78.53%). The highest user accuracy was recorded for the agriculture class (96.48%). Producer accuracy (%) rates were found as 88.41% for coniferous forest, 95.39% for broad-leaved forest, 92.57% for mixed forest, 79.06% for settlement, 92.69% for agriculture, and 85.83% for water. The highest producer accuracy was seen for the broad-leaved forest class.

The overall accuracy rate was 89.01%, and the Kappa coefficient was 0.84 for the 2020 LULC map. Producer accuracy rates for each class in the 2019 LULC map were found for coniferous forest as 77.70%, broad-leaved forest 90.66%, mixed forest 91.46%, settlement area 73.89%, agricultural land 92.28%, and water 69%. User accuracy (%) rates were above 80% for all classes except the settlement area (54.84%), with the highest user accuracy value belonging to the water class (90.78%).

When the above values were examined, it was thought that the reason for the low user and producer accuracy rates of the settlement and water classes in all periods was because they were the least represented classes within the total area. The settlement area represented 6% of the study area in all periods, whereas the water class had a ratio of 1% on the 2000 and 2010 LULC maps and 2% on the 2020 map (Fig. 5).

The Kappa value (Congalton, 2001), along with the reference data in the image classification, indicated that the accuracy of the map value was between −1 and +1 for each LULC map in this study. A Kappa coefficient of ≤ 0 means there is no fit, 0–0.2 a slight fit, 0.2–0.41 an average fit, 0.41–0.60 a moderate to intermediate level of fit, 0.60–0.80 a significant fit, and 0.81–1.0 a perfect fit. The Kappa value of 0.81–1.0 for each period classified in the study demonstrates that the classification was carried out with a perfect fit.

Table 3 LULC transition probability matrices for the 2000–2020 period of the study area

Years	2010						
	Classes	**Coniferous**	**Broad-leaved**	**Mixed**	**Settlement**	**Agriculture**	**Water**
2000	**Coniferous**	0.4722	0.1944	0.2258	0.0176	0.0779	0.0121
	Broad-leaved	0.0809	0.4780	0.2423	0.0335	0.1583	0.0070
	Mixed	0.2152	0.2714	0.4786	0.0141	0.0156	0.0050
	Settlement	0.0199	0.0441	0.0214	0.8175	0.0871	0.0100
	Agriculture	0.0726	0.2510	0.0276	0.1201	0.5083	0.0204
	Water	0.0743	0.1201	0.0377	0.2181	0.3522	0.1976
Years	**2020**						
	Classes	**Coniferous**	**Broad-leaved**	**Mixed**	**Settlement**	**Agriculture**	**Water**
2010	**Coniferous**	0.4539	0.2267	0.1658	0.0155	0.1263	0.0119
	Broad-leaved	0.0807	0.4454	0.1624	0.0348	0.2680	0.0087
	Mixed	0.2074	0.2335	0.5041	0.0177	0.0311	0.0062
	Settlement	0.0090	0.0399	0.0218	0.8335	0.0832	0.0126
	Agriculture	0.0458	0.2246	0.0333	0.1405	0.5296	0.0261
	Water	0.1137	0.0982	0.1727	0.2338	0.2719	0.1095
Years	**2020**						
	Classes	**Coniferous**	**Broad-leaved**	**Mixed**	**Settlement**	**Agriculture**	**Water**
2000	**Coniferous**	0.5858	0.0830	0.2999	0.0058	0.0092	0.0163
	Broad-leaved	0.0457	0.6487	0.2112	0.0191	0.0683	0.0070
	Mixed	0.1068	0.2426	0.6334	0.0086	0.0023	0.0063
	Settlement	0.0210	0.0557	0.0082	0.8189	0.0739	0.0223
	Agriculture	0.0632	0.3109	0.0159	0.0595	0.5288	0.0218
	Water	0.1028	0.0621	0.0058	0.1852	0.2406	0.4035

CA-Markov scenario modeling

In the study, the transition probability values for the coniferous forest, broad-leaved forest, mixed forest, settlement, agriculture, and water classes were calculated from the LULC maps as a result of the 2000–2010 supervised classification, and the 2020 LULC map was predicted. In the prediction of the 2020 and 2030 LULC maps, the number of iterations was determined as 10 and in the prediction of the 2040 LULC map, it was determined as 20, and then, estimation processes were carried out. In their study, Zadbagher et al. (2018) also set the number of iterations as 10 and 20, respectively, when estimating 2016 and 2036 LULC maps.

By using the 2010–2020 LULC transition probability matrix values, the 2030 LULC simulation maps were produced, and using the 2000–2020, LULC transition probability matrix values, LULC simulation maps up to 2040 were produced (Table 3; Fig. 6).

In Table 3, the rows represent the values of the land cover classes belonging to the previous period, and the columns represent the values for the following period. The diagonal values indicate the probability of persistence of each class, that is, the resistance of a land-cover class to move to another class, whereas values other than diagonal indicate the probability of transition from one class to another. When all the periods were examined, it was determined that the class most resistant to change was the settlement area.

Accuracy evaluation of CA–Markov model

In order to evaluate the predictive performance of the CA–Markov model used in the study, the simulated 2020 LULC map was overlapped with the reference pixels (region of interest—ROI) used in the classification for 2020, and the accuracy assessment and error matrix values were calculated (Table 4). The

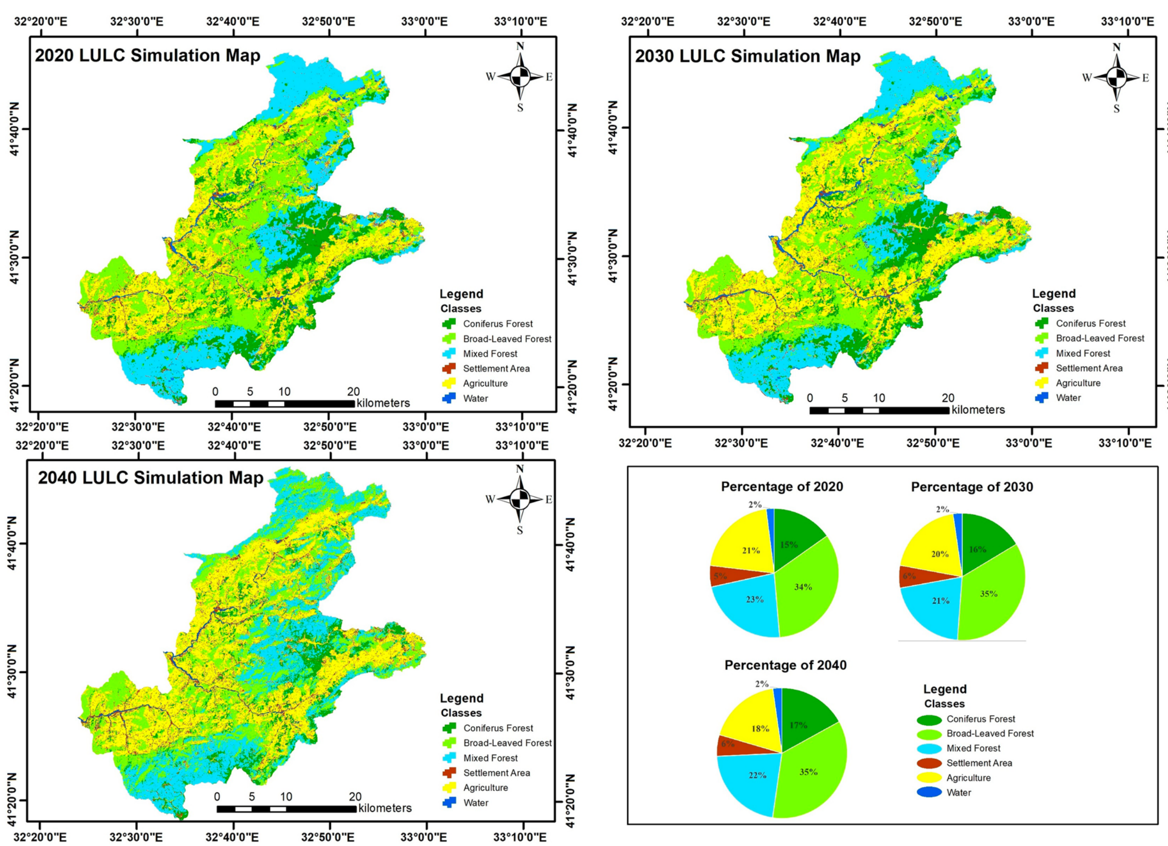

Fig. 6 LULC maps for the years 2020, 2030, and 2040 produced with the Cellular Automata-Markov model

Table 4 2020 simulated LULC map accuracy and error matrix values

2020	Coniferous	Broad-leaved	Mixed	Settlement	Agriculture	Water	Total	User´s accuracy (%)
Coniferous	18,884	217	4,199	6,499	398	12	30,209	62.51
Broad-Leaved	423	34,374	1,144	12,010	1,036	251	49,238	69.81
Mixed	1711	468	58,105	4341	31	15	64,671	89.85
Settlement	0	0	42	84,250	0	0	84,292	99.95
Agriculture	563	875	1,340	11,749	20,993	1,763	37,283	56.31
Water	17	59	693	1,504	292	2,187	4,752	46.02
Total	21,598	35,993	65,523	120,353	22,750	4,228	270,445	–
Producer´s accuracy (%)	87.43	95.50	88.68	70.00	92.28	51.73	–	–
Overall accuracy = 80.901%; Kappa coefficient 0.74								

predicted LULC map and the supervised classified LULC map for the year 2020 are shown in Fig. 7.

The simulated LULC for the year 2020 had an overall accuracy rate of 80.91% and the Kappa coefficient was 0.74. The 0.74 Kappa value of the model indicated that the model was significantly similar to the 2020 classified LULC map, and the overall accuracy of 80.90% demonstrated that at this rate, the model was reliable and usable. Model validation showed that the CA-Markov exhibited good potential

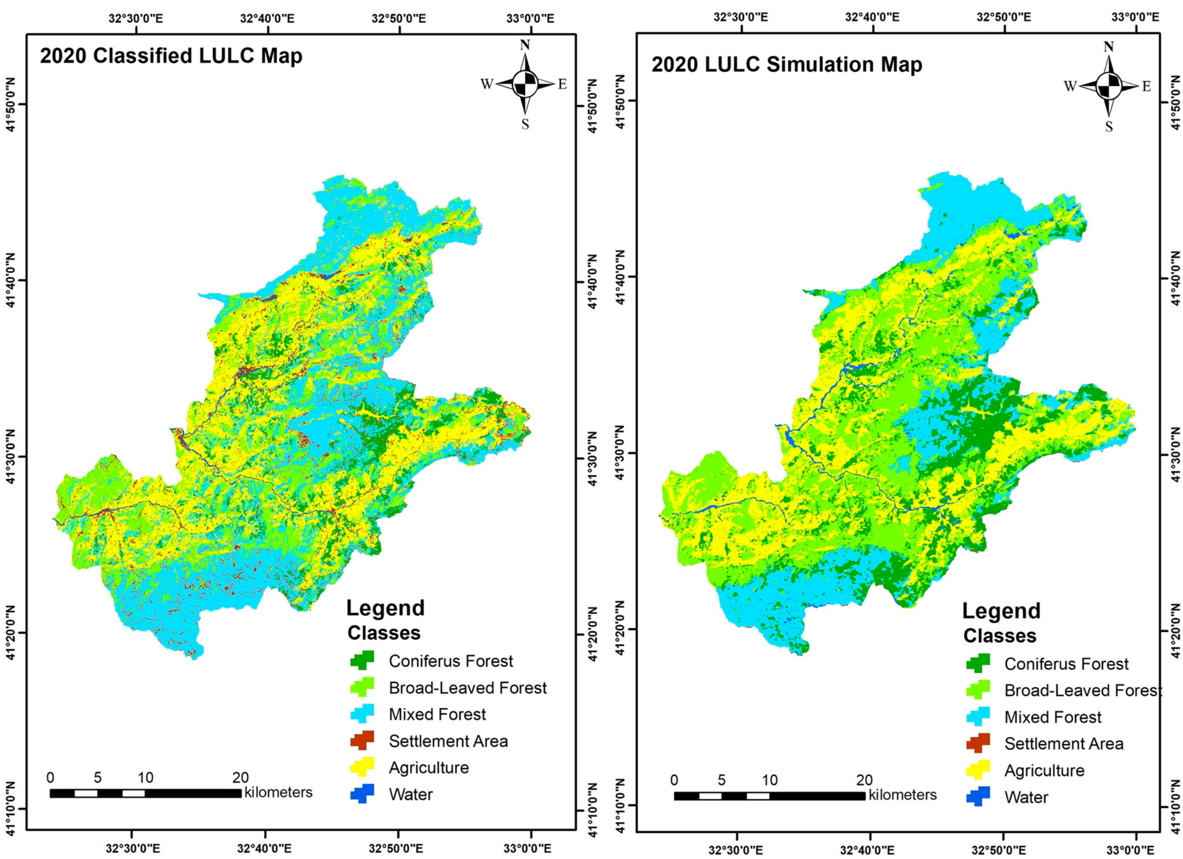

Fig. 7 Classified and simulated LULC maps of 2020

to predict future LULC changes (Table 4). Similarly, Xu et al. (2019); Feng et al. (2018); Naboureh et al. (2017); Yang et al. (2015), and Moradi et al. (2020) confirmed that the model was serviceable in their studies. The overlap graph of the areal values of the 2020 classified and simulated LULC maps is shown in Fig. 8.

LULC changes in the time intervals 2000–2020 and 2020–2040

A LULC change analysis was carried out for an area of 112,460.22 ha. The amount of land (ha) in each class was determined by dividing the LULC into six classes as coniferous, mixed, broad-leaved, settlement, agriculture, and water (Table 5). The LULC areas for each year were calculated according to the supervised classification of the 2000–2010–2020 Landsat images. The 10-year change probabilities between 2010 and 2020 were then used to predict the 2030 LULC change amount, and the 20-year change probabilities between 2000 and 2020 to predict the 2040 LULC change amount (Table 5). Although more than 50% of the total area consisted of forest in all period years, the area having the widest distribution after forest was the agricultural class. The water class was the one with the lowest area in each period (Table 5; Fig. 9).

The general forest area increased by 10,656.4 ha in 20 years (2000–2020), an increase of 15.4%, whereas the general non-forest area decreased by 24.5%. Among all classes, the highest increase rate was that of the broad-leaved forest, with 26.6%, followed by water with 68.5%, and coniferous forest with 24.9%. Of all the classes, agriculture was the only class whose land amount steadily decreased. In the intervening 20 years, it had decreased by 32.3% (11,553.9 ha).

In the Forest Class, the coniferous, broad-leaved, and mixed forest areas had increased in the 20 years by 24.9% (2,511.4 ha), 26.6% (8,116.9 ha), and 0.1% (28.1 ha), respectively. The coniferous forest area constituted 14.6% of the overall area in 2000. It increased by 5.9% in 2010 to 20.5%, whereas in 2020, by decreasing 4.7% compared to the previous period, it represented a decrease of 15.8%. The broad-leaved forest area represented 44.2% of the study area in 2000, but it increased by 1.2% in 2010, representing 45.4%. In 2020, it increased by 3.1% for a total representation of 48.5%. It was determined that the mixed forest area represented 41.1% in 2000, decreased to 34% in 2010, and finally, with an increase of 1.7% in 2020, represented 35.7%. In the Non-Forest Class, in 20 years, the agriculture and settlement areas decreased by 32.3% and 0.5%, respectively, whereas the water area increased by 68.5%. In connection with the increase in forest areas and the decrease in agricultural areas, the resulting decline in agricultural irrigation was thought to contribute to the increase of underground water resources. It is clear that the 11,553.9 ha reduction in the agriculture area was

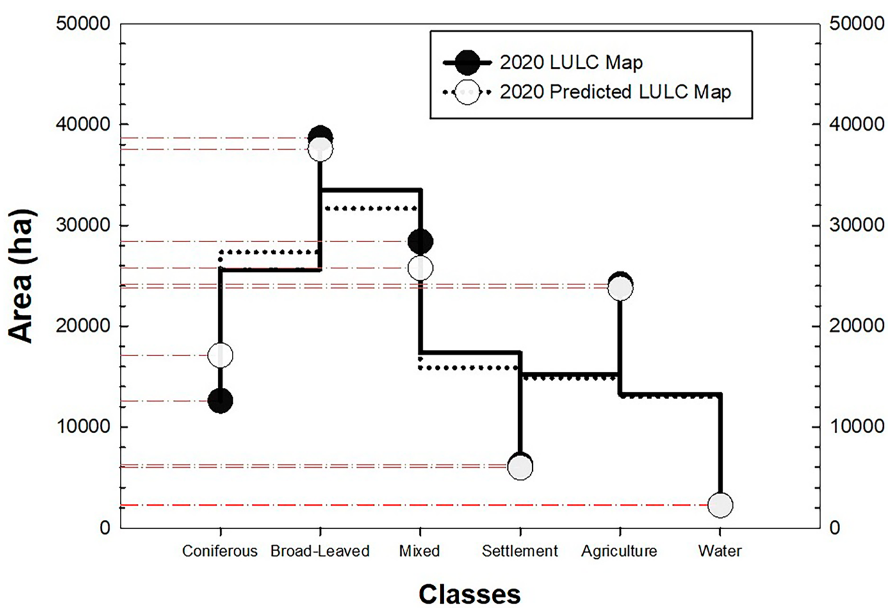

Fig. 8 Overlap graph of the simulated (predicted) 2020 LULC map with the 2020 supervised classified terrestrial LULC map

Table 5 LULC field values (ha) for the periods 2000–2010–2020–2030–2040

	Year	Area	Land use classes							
			Forest				Non-Forest			
			Coniferous	Broad-leaved	Mixed	Total	Settlement	Agriculture	Water	Total
Supervised Classified LULC Images	**2000**	**ha**	10,105.2	30,533.2	2,839.7	69,029.1	6,324.6	35,746.2	1360.1	43,430.9
		%	14.6	44.2	41.1	100	14.6	82.3	3.1	100
	2010	**ha**	15,334.7	33,923	25,386.6	74,644.2	6,607	29,625.9	1583.2	37,816
		%	20.5	45.4	34	100	17.5	78.3	4.2	100
	2020	**ha**	12,616.6	38,650	28,418.9	79,685.5	6,290	24,192.3	2292.4	32,774.7
		%	15.8	48.5	35.7	100	19.2	73.8	7.0	100
20 years of change (2000–2020)		**ha**	2511.4	8,116.9	28.1	10,656.4	−34.6	−11,553.9	932.3	−10,656.2
		% (±)	24.9	26.6	0.1	15.4	−0.5	−32.3	68.5	−24.5
Predicted LULC Maps	**2020**	**ha**	17,107.8	37,591.2	25,770.3	80,469.2	5,994.4	23,752.3	2244.3	31,991
		%	21.3	46.7	32	100	18.7	74.2	7	100
	2030	**ha**	18,455.8	39,118.7	23,564.6	81,139.1	6,458.8	22,249.3	2613	31,321.1
		%	22.7	48.2	29	100	20.6	71	8.3	100
	2040	**ha**	19,097.1	39,706.5	24,697.4	83,501	5,679	20,444.3	2836	28,959.2
		%	22.9	47.6	29.6	100	19.6	70.6	9.8	100
20 years of change (2020–2040)		**ha**	1,989.3	2,115.3	−1,072.9	3,031.8	−315.4	−3,308.1	591.7	−3,031.8
		% (±)	11.6	5.6	−4.2	3.8	−5.3	−13.9	26.4	−9.5

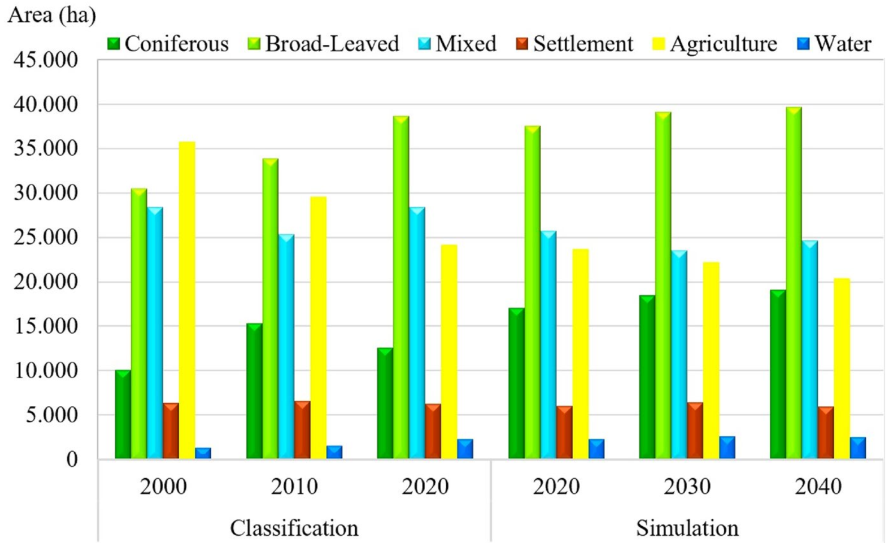

Fig. 9 LULC change for all periods (ha)

shared among all the other areas, and the vast majority of this share went to the categories within the Forest Class.

According to the predicted results obtained from the CA–Markov model for the 2020–2040 period (Table 5), in 2040, 74.24% of the general area will be Forest and 25.76% will be Non-Forest. Moreover, it was predicted that 22.9% of the Forest area would be coniferous, 47.6% broad-leaved, and 29.6% mixed forest, and 19.6% of the Non-Forest area would be settlement, 70.6% agriculture, and 9.8% water areas.

According to the 20-year (2020–2040) predicted LULC change results obtained from the CA–Markov model, it was predicted that there could be an increase of 3.8% (3031.8 ha) in the total Forest area, and a decrease of 9.5% (3031.8 ha) in the Non-Forest area. It was thought that the highest increase among the categories in the Forest Class would be in the coniferous forest category, with 11.6% (1989.3 ha), and the highest increase in the Non-Forest area would occur in the water class, with 26.4%. It was predicted that the agriculture class, which was expected to decrease continuously in all years, would decrease by 13.9% (3,308.1 ha) by the end of the 20-year period.

Discussion

Using RS, GIS, and CA-Markov models together, this study examined the LULC changes in Ulus OİS over the last 20 years (2000–2020), made LULC predictions for 2030 and 2040, and investigated possible LULC changes for the 20-year period covering the years 2020–2040. The LULC changes were examined under two separate categories: Forest and Non-Forest areas. The results were evaluated for a total of six classes: three in the Forest areas in terms of dominant tree species (coniferous, broad-leaved, and mixed forest), and three in the Non-Forest areas, as settlement, agriculture, and water.

2000–2020 LULC

The results obtained showed significant changes in LULC in the first 20 years (2000–2020). The forest area, which had been 69,029.1 ha, had increased by 15.4% to 79,685.5 in 2020, whereas a decrease of 32.3% (11,553.9 ha) was determined in the agricultural areas. Similarly, according to Kadioğullari et al. (2014); Bozali et al. (2015); Kaptan and Durkaya, (2019) and Kaptan et al. (2019) in their studies on land change, there has been a decrease in agricultural areas for some regions of Turkey (Kaptan, 2021b). Agricultural areas have tended to decrease in Turkey in general over the last 85-year period covering 1949–2015 (Bayar, 2018). The settlement areas had decreased by the very small rate of 0.5%, whereas the water areas had increased by 68.5%. Results from the study showed that the greatest number of transformations had occurred between the agriculture and forest areas. The decrease in agricultural irrigation in connection with the increase in forest areas and the decrease in agricultural areas was thought to have contributed to an increase of groundwater resources.

Most of the settlement areas in the study are located in or bordering forests that are widely distributed on sloping and mountainous lands. Because of the physical features of the terrain and the character of the inhabitants, the local people living here and referred to as "forest villagers" lack many opportunities in socio-economic terms compared to those living in the city. Therefore, from past to present, there has been an intense migration from rural areas to the cities. The population of the forest villages in the study area decreased by 64.64% according to the 1960–2010 district-based average population changes in Bartın Province forest villages, which shows that the forest villages of Ulus district had the highest decrease among the forest villages of Bartın (Günşen, 2012; Kaptan & Durkaya, 2019). Due to the decreasing population, the social pressure on forest areas has eased, and with the arrival and development of forest tree seeds on abandoned agricultural lands, forests have begun to grow again in these areas (Başkent & Kadioğullari, 2007; Sivrikaya et al., 2007; Çakir et al., 2008; Kadioğullari et al., 2008; Reis et al., 2016; Kaptan, 2018, 2021a). In addition, the successful forestry and afforestation works carried out throughout the country from the past to the present in line with the mission and objectives of the General Directorate of Forestry have made a great contribution to the expansion of forest areas.

Population growth in urban areas is associated with high birth rates as well as migration from rural to urban areas (Mansour et al., 2020). With the migration from the countryside to the city, the problems in the countryside have also moved to the cities. In order to reduce the population density and problems experienced in the cities and to improve the production of agricultural products and animal husbandry, the government has introduced various incentives to initiate a reverse migration movement from the cities to the countryside. The results of these strategies are not currently at the expected level for the study area, and the migration movement toward the city centers still continues. Therefore, under these conditions, improvement and expansion of the agricultural land in the study area does not seem very likely.

2020–2040 LULC simulation

In this study, LULC changes in the study area were successfully simulated via the integration of remote sensing and GIS techniques with the CA–Markov model. When predicting the future, the model simulates the type of change in the periods specified by the transition probability values it has created for each class, based on the changes in the classes for the determined periods (Table 3). The realization of the changes in the 2000–2020 period and the possible expectations for the 2020–2040 period, in direct proportion to each other, arise from the working principle of the model. The reliability of the CA–Markov model was verified with reference data for the years 2000 and 2010 (Table 4). The neighborhood factor in the model was the most important factor in generating terrain suitability maps for each LULC class.

The results of the CA–Markov model simulation also clearly showed that in 2030 and 2040, agricultural land would shrink, and the forest and water areas would continue to expand. Aksoy and Kaptan (2020), in a study in which they estimated the LULC for 2019 and 2039 for a specified part of Bartın Province using the CA–Markov model, predicted that forest, settlement, and water areas would increase and agricultural areas decrease, as in the current findings. Using the CA–Markov model, Bozkaya et al. (2015) simulated a land-use model for the Iğneada conservation area of Turkey in 2030, which revealed that agricultural lands and barren areas would gradually become forested, and accordingly, forest areas would increase. By estimating the possible LULC changes up to the year 2036 in the Seyhan basin of Turkey using the CA–Markov model, Zadbagher et al. (2018) predicted that the residential areas would increase and the forest areas would decrease in the study area. The emergence of diverse results in these studies can be attributed to the economic, ecological, and sociocultural differences of each study area.

The model predicted that the highest increase in the Forest category, which was expected to increase in the 2020–2040 period, would be in the coniferous forest class, and the greatest decrease would be in the agriculture class in the Non-Forest area category. Although the water class had the lowest rate among all classes, its predicted increase was thought to be related to the expanding of forest areas as well as to the shrinking of agricultural areas because the abandonment of agricultural areas, especially resulting from the decreasing population, would lead to reduced agricultural irrigation. Accordingly, if the situation of agricultural lands continues in this way in the future, it will contribute to the increase of underground water resources, and thus, it is expected that the water class will continue to expand. Compared to other land uses like urbanized areas or arable land, forests offer lower runoff (Adhikari et al., 2002; Fiquepron et al., 2013; Sikka & Selvi, 2005). The areal expansion experienced or likely to be experienced in the forest areas will feed the underground water resources by reducing the precipitation regime and lowering the transmission of precipitation waters to the surface flow. It is thought that this will contribute naturally to the increase of visible water resources.

Conclusion

Assessment of the LULC can assist managers, policy-makers, and planners in making more reliable decisions about sustainable management of land and resources. Because of their high image processing capabilities, GIS satellite imagery and RS techniques are widely used in the production of LULC maps and in the management of natural resources, especially those of forest and water.

The results showed that the integration of RS, GIS, and simulation models can be used successfully in monitoring, predicting, mapping, and reporting changes in LULC. The integration of RS, GIS, and simulation models can contribute to effective planning and management of natural resources such as forests, to regulation of agricultural policies, to the understanding of the driving forces of LULC changes, to providing necessary precautions in advance, and thus, to more correct decision-making within the scope of sustainable development. The point to be considered here, especially in terms of forestry policy, is the creation of the best forest type that would enable achievement of the goals and targets determined within the scope of the purpose-function relationship because the products, benefits, and services offered by each type of forest (broad-leaved, coniferous, and mixed) differ. For example, broad-leaved forests cannot contribute as much as coniferous forests to the production of potable-quality water. Many other examples can be given, such as the fact that broad-leaved forests are more resistant to fire than coniferous forests, and that mixed forests accommodate a rich biodiversity.

For general forest areas, the temporal and spatial changes in coniferous, mixed, and broad-leaved forest classes should be examined in terms of quality and quantity. However, the effects and intensities of natural (storm, fire, insect damage, etc.) or human interventions, as well as topographic, edaphic, and climatic factors, which are all thought to have possible effects on the changes experienced, should be analyzed by spatially integrating them with decision support systems for severity. Revealing the impact and severity of the factors subject to change would provide the opportunity to evaluate the events and results more accurately as well as the opportunity for decision-makers and planners to intervene at the right place and time.

Acknowledgements We would like to thank the General Directorate of Forestry (Orman Genel Müdürlüğü—OGM), the Zonguldak Regional Directorate of Forestry, and the Ulus Directorate of Forest Operations and their staff for supplying and delivering the forest cover–type maps and forest management plans.

Data availability All data generated or analyzed during this study are included in this published article (and its supplementary information files).

References

Aburas, M. M., Ho, Y. M., Pradhan, B., Salleh, A. H., & Alazaiza, M. Y. (2021). Spatio-temporal simulation of future urban growth trends using an integrated CA-Markov model. *Arabian Journal of Geosciences, 14*(2), 1–12. https://doi.org/10.1007/s12517-021-06487-8

Adhikari, R. N., Rao, M. S. R. M., Selvi, V., Math, S. K. N., Husenappa, V., Chandrappa, M., & Reddy, K. K. (2002). Studies on runoff coefficient of rational formula. *Indian Journal of Soil Conservation, 30*(1), 106–108.

Akinyemi, F. O. (2017). Land change in the central Albertine rift: Insights from analysis and mapping of land use-land cover change in north-western Rwanda. *Applied Geography, 87*, 127–138. https://doi.org/10.1016/j.apgeog.2017.07.016

Akinyemi, F. O., Pontius, R. G., Jr., & Braimoh, A. K. (2017). Land change dynamics: Insights from Intensity Analysis applied to an African emerging city. *Journal of Spatial Science, 62*(1), 69–83. https://doi.org/10.1080/14498596.2016.1196624

Aksoy, H., & Kaptan, S. (2020). Simulation of future forest and land use/cover changes (2019–2039) usingthe cellular automata-Markov model. *Geocarto International*, 1-20. https://doi.org/10.1080/10106049.2020.1778102

Anon. (2020). Bartın Valiliği Web Sayfası. http://www.bartin.gov.tr

Atik, S. (1998). Bartın İl Turizm Envanteri ve Turizmi Geliştirme Planı Açıklama Raporu. *Bartın Valiliği, Bartın*, 150 s.

Ball, G. L. (1994). Ecosystem modeling with GIS. *Environmental Management, 18*(3), 345–349. https://doi.org/10.1007/BF02393865

Başkent, E. Z., & Kadioğullari, A. I. (2007). Spatial and temporal dynamics of land use pattern in Turkey: A case study in İnegöl. *Landscape and Urban Planning, 81*(4), 316–327. https://doi.org/10.1016/j.landurbplan.2007.01.007

Bayar, R. (2018). Arazi kullanımı açısından Türkiye'de tarım alanlarının değişimi. *Coğrafi Bilimler Dergisi, 16*(2), 187–200.

Bozali, N., Sivrikaya, F. & Akay, A.E. (2015). Use of spatial pattern analysis to assess forest cover changes in the Mediterranean region of Turkey. *Journal of Forest Research*, *20*, 365–374. https://doi.org/10.1007/s10310-015-0493-2

Bozkaya, A. G., Balcik, F. B., Goksel, C., & Esbah, H. (2015). Forecasting land-cover growth using remotely sensed data: A case study of the Igneada protection area in Turkey. *Environmental Monitoring and Assessment, 187*(3), 1–18. https://doi.org/10.1007/s10661-015-4322-z

Carpenter, S. R., Mooney, H. A., Agard, J., Capistrano, D., DeFries, R. S., Díaz, S., Dietz, T., Duraiappah, A. K., Oteng-Yeboah, A. A., Perrings, C., Reid, W. V., Sarukhan, J., Pereira, H. M., Scholes, R. J., & Whyte, A. (2009). Science for managing ecosystem services: Beyond the Millennium Ecosystem Assessment. *Proceedings of the National Academy of Sciences, 106*(5), 1305–1312. https://doi.org/10.1073/pnas.0808772106

Congalton, R. G. (2001). Accuracy assessment and validation of remotely sensed and other spatial information. *International Journal of Wildland Fire, 10*(4), 321–328. https://doi.org/10.1071/WF01031

Congalton, R. G., Green, K. (2019). *Assessing the accuracy of remotely sensed data: principles and practices (3rd Ed.).* CRC press

Çakir, G., Sivrikaya, F., & Keleş, S. (2008). Forest cover change and fragmentation using Landsat data in Macka state forest enterprise in Turkey. *Environmental Monitoring and Assessment, 137*(1–3), 51–66. https://doi.org/10.1007/s10661-007-9728-9

da Cunha, E. R., Santos, C. A. G., da Silva, R. M., Bacani, V. M., & Pott, A. (2021). Future scenarios based on a CA-Markov land use and land cover simulation model for a tropical humid basin in the Cerrado/Atlantic forest ecotone of Brazil. *Land Use Policy, 101*, 105141. https://doi.org/10.1016/j.landusepol.2020.105141

Degife, A. W., Zabel, F., & Mauser, W. (2018). Assessing land use and land cover changes and agricultural farmland expansions in Gambella Region Ethiopia using Landsat 5 and Sentinel 2a multispectral data. *Heliyon, 4*(11), e00919. https://doi.org/10.1016/j.heliyon.2018.e00919

Feng, Y., Cai, Z., Tong, X., Wang, J., Gao, C., Chen, S., & Lei, Z. (2018). Urban growth modeling and future scenario projection using cellular automata (CA) models and the R Package Optimx. *ISPRS International Journal of Geo-Information, 7*(10), 387. https://doi.org/10.3390/ijgi7100387

Feng, Y., Lei, Z., Tong, X., Gao, C., Chen, S., Wang, J., & Wang, S. (2020). Spatially-explicit modeling and intensity analysis of China's land use change 2000–2050. *Journal of Environmental Management, 263*, 110407. https://doi.org/10.1016/j.jenvman.2020.110407

Fiquepron, J., Garcia, S., & Stenger, A. (2013). Land use impact on water quality: Valuing forest services in terms of the water supply sector. *Journal of Environmental Management, 126*, 113–121. https://doi.org/10.1016/j.jenvman.2013.04.002

Gharbia, S. S., Abd Alfatah, S., Gill, L., Johnston, P., & Pilla, F. (2016). Land use scenarios and projections simulation using an integrated GIS cellular automata algorithms. *Modeling Earth Systems and Environment, 2*(3), 1–20. https://doi.org/10.1007/s40808-016-0210-y

Gómez, C., White, J. C., & Wulder, M. A. (2016). Optical remotely sensed time series data for land cover classification: A review. *ISPRS Journal of Photogrammetry and Remote Sensing, 116*, 55–72. https://doi.org/10.1016/j.isprsjprs.2016.03.008

Guan, D., Gao, W., Watari, K., & Fukahori, H. (2008). Land use change of Kitakyushu based on landscape ecology and Markov model. *Journal of Geographical Sciences, 18*(4), 455–468. https://doi.org/10.1007/s11442-008-0455-0

Günşen, H. B. (2012). *Orman köylerinde iç göçleri etkileyen faktörler (Bartın-Kastamonu Örneği).* Bartın Üniversitesi Fen Bilimleri Enstitüsü Doktora Tezi.

Hou, H., Wang, R., & Murayama, Y. (2019). Scenario-based modelling for urban sustainability focusing on changes in cropland under rapid urbanization: A case study of Hangzhou from 1990 to 2035. *Science of the Total Environment, 661*, 422–431. https://doi.org/10.1016/j.scitotenv.2019.01.208

Huang, Y., Yang, B., Wang, M., Liu, B., & Yang, X. (2020). Analysis of the future land cover change in Beijing using CA–Markov chain model. *Environmental Earth Sciences, 79*(2), 1–12. https://doi.org/10.1007/s12665-019-8785-z

Itami, R. M. (1994). Simulating spatial dynamics: Cellular automata theory. *Landscape and Urban Planning, 30*(1–2), 27–47. https://doi.org/10.1016/0169-2046(94)90065-5

Kadioğullari, A. İ, Keleş, S., Başkent, E. Z., & Günlü, A. (2008). Spatiotemporal changes in landscape pattern in response to aforestation in Northeastern Turkey: a case study of Torul. *Scottish Geographical Journal*, *124*(4), 259–273. https://doi.org/10.1080/14702540802566254

Kadioğullari, A. İ, Sayin, M. A., Çelįk, D. A., Borucu, S., Çįl, B., & Bulut, S. (2014). Analysing land cover changes for understanding of forest dynamics using temporal forest management plans. *Environmental Monitoring and Assessment, 186*(4), 2089–2110.

Kamusoko, C., Aniya, M., Adi, B., & Manjoro, M. (2009). Rural sustainability under threat in Zimbabwe–simulation of future land use/cover changes in the Bindura district based on the Markov-cellular automata model. *Applied*

Geography, 29(3), 435–447. https://doi.org/10.1016/j.apgeog.2008.10.002

Kaptan, S. (2018). *Sosyo-Ekonomik Durum Envanteri ve Orman Amenajman Planlarına Yansıtılması*. Doktora Tezi Bartın Üniversitesi Fen Bilimleri Enstitüsü

Kaptan, S. (2021a). Changes in forest areas and land cover and their causes using ıntensity analysis: The case of Alabarda Forest Planning Unit. *Environmental Monitoring and Assessment, 193*(7), 1–17. https://doi.org/10.1007/s10661-021-09089-9

Kaptan, S. (2021b). Arazi örtüsü ile meşcere gelişim çağı ve kapalılığı kategorilerindeki zamansal değişimlerin incelenmesi: Karabiga Orman İşletme Şefliği örneği. *Turkish Journal of Forestry*, *22*(2), 97-104. https://doi.org/10.18182/tjf.903733

Kaptan, S., Aksoy, H., Durkaya, B., Aksoy, Ş. Ç. (2019). Coğrafi bilgi sistemleri ile arazi örtüsü ve kullanımında yaşanan değişimlerin incelenmesi (Akgöl orman işletme şefliği örneği). 8th International Vocational Schools Symposium.

Kaptan, S., & Durkaya, A. (2019). Analysing temporal and spatial changes in land cover: the case of Drahna Forest Subdistrict Directorate. *Kastamonu University Journal of Forestry Faculty*, *19*(1), 47–56. https://doi.org/10.17475/kastorman.543428

Karki, S., Thandar, A. M., Uddin, K., Tun, S., Aye, W. M., Aryal, K., Kandel, P., & Chettri, N. (2018). Impact of land use land cover change on ecosystem services: A comparative analysis on observed data and people's perception in Inle Lake Myanmar. *Environmental Systems Research, 7*(1), 1–15. https://doi.org/10.1186/s40068-018-0128-7

Keshtkar, H., & Voigt, W. (2016). Potential impacts of climate and landscape fragmentation changes on plant distributions: Coupling multi-temporal satellite imagery with GIS-based cellular automata model. *Ecological Informatics, 32*, 145–155. https://doi.org/10.1016/j.ecoinf.2016.02.002

Keshtkar, H., Voigt, W., & Alizadeh, E. (2017). Land-cover classification and analysis of change using machine-learning classifiers and multi-temporal remote sensing imagery. *Arabian Journal of Geosciences, 10*, 154. https://doi.org/10.1007/s12517-017-2899-y

Khawaldah, H. A., Farhan, I., & Alzboun, N. M. (2020). Simulation and prediction of land use and land cover change using GIS, remote sensing and CA-Markov model. *Global Journal of Environmental Science and Management*, *6*(2), 215–232. https://doi.org/10.22034/GJESM.2020.02.07

Khwarahm, N. R. (2021). Spatial modeling of land use and land cover change in Sulaimani, Iraq, using multitemporal satellite data. *Environmental Monitoring and Assessment, 193*(3), 1–18. https://doi.org/10.1007/s10661-021-08959-6

Khwarahm, N. R., Qader, S., Ararat, K., & Al-Quraishi,A. M. F. (2020). Predicting and mapping land cover/land use changes in Erbil/Iraq using CA-Markovsynergy model. *Earth Science Informatics*, 1-14. https://doi.org/10.1007/s12145-020-00541-x

Li, W., Dong, R., Fu, H., Wang, J., Yu, L., & Gong, P. (2020). Integrating Google Earth imagery with Landsat data to improve 30-m resolution land cover mapping. *Remote Sensing of Environment, 237*, 111563. https://doi.org/10.1016/j.rse.2019.111563

Mansour, S., Al-Belushi, M., & Al-Awadhi, T. (2020). Monitoring land use and land cover changes in the mountainous cities of Oman using GIS and CA-Markov modelling techniques. *Land Use Policy, 91*, 104414. https://doi.org/10.1016/j.landusepol.2019.104414

Mondal, M. S., Sharma, N., Garg, P. K., & Kappas, M. (2016). Statistical independence test and validation of CA Markov land use land cover (LULC) prediction results. *The Egyptian Journal of Remote Sensing and Space Science, 19*(2), 259–272. https://doi.org/10.1016/j.ejrs.2016.08.001

Moradi, F., Kaboli, H. S., & Lashkarara, B. (2020). Projection of future land use/cover change in the Izeh-Pyon Plain of Iran using CA-Markov model. *Arabian Journal of Geosciences, 13*(19), 1–17. https://doi.org/10.1007/s12517-020-05984-6

Motlagh, Z. K., Lotfi, A., Pourmanafi, S., Ahmadizadeh, S., & Soffianian, A. (2020). Spatial modeling of land-use change in a rapidly urbanizing landscape in central Iran: Integration of remote sensing, CA-Markov, and landscape metrics. *Environmental Monitoring and Assessment, 192*(11), 1–19. https://doi.org/10.1007/s10661-020-08647-x

Munthali, M. G., Mustak, S., Adeola, A., Botai, J., Singh, S. K., & Davis, N. (2020). Modelling land use and land cover dynamics of Dedza district of Malawi using hybrid Cellular Automata and Markov model. *Remote Sensing Applications: Society and Environment, 17*, 100276. https://doi.org/10.1016/j.rsase.2019.100276

Naboureh, A., Moghaddam, M. H. R., Feizizadeh, B., & Blaschke, T. (2017). An integrated object-based image analysis and CA-Markov model approach for modeling land use/land cover trends in the Sarab plain. *Arabian Journal of Geosciences, 10*(12), 1–16. https://doi.org/10.1007/s12517-017-3012-2

Niya, A. K., Huang, J., Kazemzadeh-Zow, A., Karimi, H., Keshtkar, H., & Naimi, B. (2020). Comparison of three hybrid models to simulate land use changes: A case study in Qeshm Island Iran. *Environmental Monitoring and Assessment, 192*(5), 1–19. https://doi.org/10.1007/s10661-020-08274-6

Pflugmacher, D., Rabe, A., Peters, M., & Hostert, P. (2019). Mapping pan-European land cover using Landsat spectral-temporal metrics and the European LUCAS survey. *Remote Sensing of Environment, 221*, 583–595. https://doi.org/10.1016/j.rse.2018.12.001

Reddy, C. S., Saranya, K. R. L., Pasha, S. V., Satish, K. V., Jha, C. S., Diwakar, P. G., Dadhwal, V. K., Rao, P. V. N., & Murthy, Y. K. (2018). Assessment and monitoring of deforestation and forest fragmentation in South Asia since the 1930s. *Global and Planetary Change, 161*, 132–148. https://doi.org/10.1016/j.gloplacha.2017.10.007

Reis, M., Dutal, H., Abız, B., & Bolat, N. (2016). Kahramanmaraş ili Göksun ilçesinde arazi kullanımında meydana gelen zamansal değişimin uzaktan algılama teknikleri ve coğrafi bilgi sistemi ile belirlenmesi. *Kahramanmaraş Sütçü İmam Üniversitesi Mühendislik Bilimleri Dergisi*, *19*(2), 35–41. https://doi.org/10.17780/ksujes.91496

Ren, Y., Lü, Y., Comber, A., Fu, B., Harris, P., & Wu, L. (2019). Spatially explicit simulation of land use/land cover changes: Current coverage and future prospects.

Earth-Science Reviews, 190, 398–415. https://doi.org/10.1016/j.earscirev.2019.01.001

Rimal, B., Keshtkar, H., Sharma, R., Stork, N., Rijal, S., & Kunwar, R. (2019). Simulating urban expansion in a rapidly changing landscape in eastern Tarai Nepal. *Environmental Monitoring and Assessment, 191*(4), 1–14. https://doi.org/10.1007/s10661-019-7389-0

Rohde, K. (Ed.). (2013). *The Balance of Nature and Human Impact*. Cambridge University Press.

Ruben, G. B., Zhang, K., Dong, Z., & Xia, J. (2020). Analysis and projection of land-use/land-cover dynamics through scenario-based simulations using the CA-Markov model: A case study in Guanting Reservoir Basin China. *Sustainability, 12*(9), 3747. https://doi.org/10.3390/su12093747

Salem, M., Tsurusaki, N., & Divigalpitiya, P. (2020). Land use/land cover change detection and urban sprawl in the peri-urban area of greater Cairo since the Egyptian revolution of 2011. *Journal of Land Use Science, 15*(5), 592–606. https://doi.org/10.1080/1747423X.2020.1765425

Sang, L., Zhang, C., Yang, J., Zhu, D., & Yun, W. (2011). Simulation of land use spatial pattern of towns and villages based on CA–Markov model. *Mathematical and Computer Modelling, 54*(3–4), 938–943. https://doi.org/10.1016/j.mcm.2010.11.019

Schulp, C. J., Nabuurs, G. J., & Verburg, P. H. (2008). Future carbon sequestration in Europe—effects of land use change. *Agriculture, Ecosystems & Environment, 127*(3–4), 251–264. https://doi.org/10.1016/j.agee.2008.04.010

Sikka, A. K., & Selvi, V. (2005). Experimental examination of rational runoff coefficient for small agricultural and forest watersheds in the Nilgiris. *IE (I) Journal—AG*.

Singh, S. K., Mustak, S., Srivastava, P. K., Szabó, S., & Islam, T. (2015). Predicting spatial and decadal LULC changes through cellular automata Markov chain models using earth observation datasets and geo-information. *Environmental Processes, 2*(1), 61–78. https://doi.org/10.1007/s40710-015-0062-x

Sivrikaya, F., Çakır, G., Kadioğullari, A., Keleş, S., Başkent, E. Z., & Terzioğlu, S. (2007). Evaluating land use/land cover changes and fragmentation in the Camili forest planning unit of northeastern Turkey from 1972 to 2005. *Land Degradation & Development, 18*(4), 383–396. https://doi.org/10.1002/ldr.782

Snedecor, G., & Cochran, W. (1969). Statistical methods 6th ed The Iowa State University Press Ames lowa USA.

Steffen, W., Sanderson, R. A., Tyson, P. D., Jäger, J., Matson, P. A., Moore III, B., Oldfield, F., Richardson, K., Schellnhuber, H. J., Turner, B. L., & Wasson, R. J. (2006). *Global change and the earth system: a planet under pressure*. Springer Science & Business Media.

Tolessa, T., Senbeta, F., & Kidane, M. (2017). The impact of land use/land cover change on ecosystem services in the central highlands of Ethiopia. *Ecosystem Services, 23*, 47–54. https://doi.org/10.1016/j.ecoser.2016.11.010

USGS, (2020). *United States Geological Survey Landsat Missions Landsat 8*. Accessed November 06, 2020, from https://www.usgs.gov/

Verburg, P. H., & Overmars, K. P. (2009). Combining top-down and bottom-up dynamics in land use modeling: Exploring the future of abandoned farmlands in Europe with the Dyna-CLUE model. *Landscape Ecology, 24*(9), 1167–1181. https://doi.org/10.1007/s10980-009-9355-7

Wang, R., & Murayama, Y. (2017). Change of land use/cover in Tianjin city based on the markov and cellular automata models. *ISPRS International Journal of Geo-Information, 6*(5), 150. https://doi.org/10.3390/ijgi6050150

Wang, Y., & Zhang, X. (2001). A dynamic modeling approach to simulating socioeconomic effects on landscape changes. *Ecological Modelling, 140*(1–2), 141–162. https://doi.org/10.1016/S0304-3800(01)00262-9

Weng, Q. (2002). Land use change analysis in the Zhujiang Delta of China using satellite remote sensing GIS and stochastic modelling. *Journal of Environmental Management, 64*(3), 273–284. https://doi.org/10.1006/jema.2001.0509

Wolfram, S. (1984). Cellular automata as models of complexity. *Nature, 311*(5985), 419–424. https://doi.org/10.1038/311419a0

Wu, X., Shen, Z., Liu, R., & Ding, X. (2008). Land use/cover dynamics in response to changes in environmental and socio-political forces in the upper reaches of Yangtze River China. *Sensors*, *8*(12), 8104–8122. https://doi.org/10.3390/s8128104

Xu, T., Gao, J., & Coco, G. (2019). Simulation of urban expansion via integrating artificial neural network with Markov chain–cellular automata. *International Journal of Geographical Information Science, 33*(10), 1960–1983. https://doi.org/10.1080/13658816.2019.1600701

Yang, Y., Zhang, S., Yang, J., Xing, X., & Wang, D. (2015). Using a cellular automata-Markov model to reconstruct spatial land-use patterns in Zhenlai County northeast China. *Energies, 8*(5), 3882–3902. https://doi.org/10.3390/en8053882

Zadbagher, E., Becek, K., & Berberoglu, S. (2018). Modeling land use/land cover change using remote sensing and geographic information systems: Case study of the Seyhan Basin Turkey. *Environmental Monitoring and Assessment, 190*(8), 1–15. https://doi.org/10.1007/s10661-018-6877-y

Zhu, Z., & Woodcock, C. E. (2014). Continuous change detection and classification of land cover using all available Landsat data. *Remote Sensing of Environment, 144*, 152–171. https://doi.org/10.1016/j.rse.2014.01.011